Atienzar Corvillo, PE.; De Victoria-Rodriguez, M.; Juanes, O.; Rodríguez-Ubis, J.; Brunet, E.; García Gómez, H. (2011). Layered gamma-zirconium phosphate as novel semiconductor for dye sensitized solar cells: Improvement of photovoltaic efficiency by intercalation of a ruthenium complex-viologen dyad. Energy and Environmental Science. 4(11):4718-4726. doi:10.1039/C1EE02158C

Layered g-zirconium phosphate as novel semiconductor for dye sensitized solar cells: Improvement of photovoltaic efficiency by intercalation of a ruthenium complex-viologen dyad

Pedro Atienzar, Mar´ıa de Victoria-Rodriguez, Olga Juanes, Juan Carlos Rodr´ıguez-Ubis, Ernesto Brunet* and Hermenegildo Garc´ıa*

A dye sensitized solar cell based on the inclusion of a ruthenium dye inside the intergallery space of layered g-zirconium phosphate has been built.

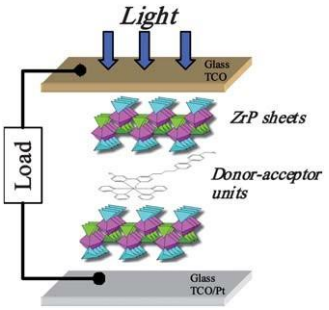

Please check this proof carefully. **Our staff will not read it in detail after you have returned it.**

Translation errors between word-processor files and typesetting systems can occur so the whole proof needs to be read. Please pay particular attention to: tabulated material; equations; numerical data; figures and graphics; and references. If you have not already indicated the corresponding author(s) please mark their name(s) with an asterisk. Please e-mail a list of corrections or the PDF with electronic notes attached – do not change the text within the PDF file or send a revised manuscript.

Please bear in mind that minor layout improvements, e.g. in line breaking, table widths and graphic placement, are routinely applied to the final version.

We will publish articles on the web as soon as possible after receiving your corrections; no late corrections will be made.

Please return your **final** corrections, where possible within **48 hours** of receipt by e-mail to: ees@rsc.org

Reprints—Electronic (PDF) reprints will be provided free of charge to the corresponding author. Enquiries about purchasing paper reprints should be addressed via: http://www.rsc.org/publishing/journals/guidelines/paperreprints/. Costs for reprints are below:

Reprint costs

No of pages	Cost (per 50 copies)	
	First	Each additional
2–4	£225	£125
5–8	£350	£240
9–20	£675	£550
21–40	£1250	£975
>40	£1850	£1550

Cost for including cover of journal issue:
£55 per 50 copies

Layered g-zirconium phosphate as novel semiconductor for dye sensitized solar cells: Improvement of photovoltaic efficiency by intercalation of a ruthenium complex-viologen dyad†

Pedro Atienzar,[a] María de Victoria-Rodriguez,[b] Olga Juanes,[b] Juan Carlos Rodríguez-Ubis,[b] Ernesto Brunet*[b] and Hermenegildo García*[a]

Received 16th July 2011, Accepted 7th September 2011
DOI: 10.1039/c1ee02158c

The performance of photovoltaic cells using as semiconductor a film of layered g-zirconium phosphate (g-ZrP) containing $Ru(bpy)_3$ and bipyridinium ions (viologens) as electron relays has been studied. The materials are easily prepared by intercalation of Ru complexes and the bipyridinium ions into preformed g-ZrP nano sheets as colloidal solutions in the appropriate solvent and concentration. High loading of these two guests has been obtained as determined by elemental analysis. Inclusion of Ru $(bpy)_3$ complex and bipyridinium in the intergallery spaces of g-ZrP can be assessed by powder XRD monitoring of the d_{100} peak. A dyad was also synthesized where the $Ru(bpy)_3$ and the 4,4′-bipyridinium were covalently connected by a four-methylene tether. The semiconducting behavior of layered g-ZrP was supported by cyclic voltammetry (reversible reduction peak at —0.6 V), observation of photocurrent and Mott-Schottky measurements (flat band potential ~—1.3 V *vs.* NHE) of thin films of this material supported on FTO electrode. Photovoltaic cells based on g-ZrP containing $Ru(bpy)_3$, exhibited similar V_{OC} (~0.5 V) and fill-factor values (0.3–0.4), differing in the current density and therefore in their efficiency. The maximum efficiency was obtained for the material containing high loading of the dyad (J_{SC} ¼ 0.383 mA/cm^2, efficiency 0.1%). The photo response spectrum shows that the main limitation of these materials is still the inefficient photo sensitization of the semiconductor by the dye, probably due to the high negative flat band potential of g-ZrP.

Introduction

Virtually all dye sensitized solar cells (DSSCs) are based on titanium dioxide acting as semiconductor.[1] However, since Grätzel's initial reports on the photovoltaic activity of nano- porous titanium dioxide films[2] and, after numerous studies in this field, 10% efficiency appears to be an insurmountable limit with the current know-how concerning titania-based DSSCs.[3] It could

[a]*Instituto Universitario de Tecnología Química UPV-CSIC, Universidad Politécnica de Valencia, Av. de los Naranjos s/n, Valencia, Spain. E-mail: hgarcia@qim.upv.es; Fax: +34 96387 7809; Tel: +34 96387 7807*
[b]*Departamento de Química Orgánica, Facultad de Ciencias, Universidad Autónoma de Madrid, 28049 Madrid, Spain. E-mail: ernesto.brunet@uam.es; Fax: +34 91497 3966; Tel: +34 91497 3926*

† Electronic supplementary information (ESI) available. See DOI: 10.1039/c1ee02158c

Broader context

Dye sensitized solar cells are expected to play a key role in solar energy conversion into electricity. Titania is the almost exclusive semiconductor employed in this type of photovoltaic devices. The maximum efficiency of titania-based solar cells is about 10% and this value is still not sufficiently high for bringing these devices into commercial. However, in spite of the intensive research in this area the success in increasing the quantum efficiency has been so far unsuccessful. In this context, it would of interest to explore the behavior of other semiconductors. Herein, we report a photovoltaic cell based on a totally different semiconductor that consists in layers of g-zirconium phosphate. The beauty of our system is that in the intergallery spaces of this layered material we have incorporated a photoactive ruthenium complex, ensuring a good interfacial contact between the photosensitizing dye and the semiconductor. Although the overall efficiency is still far from reaching the values currently achieved with titanium dioxide, our report opens the way for further research in this area trying to increase the overall efficiency, a possibility that can derive from the use of a more suitable dye, higher light absorption, doping of the semiconductor or other modifications of the system.

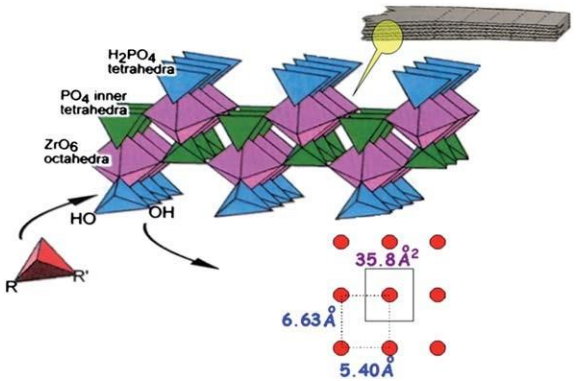

Fig. 1 Polyhedral model of a portion of one layer of g-ZrP, showing the topotactic exchange process and the available area around every surface phosphate.

then be advisable to explore other materials or semiconductors that so far exhibit promising efficiencies which, by way of simple structural changes, might achieve similar or even higher quantum efficiencies than those of the TiO_2-based composites and, therefore, they could become an alternative to them. From the structural point of view layered zirconium phosphates (g-ZrP), bear quite a remarkable degree of versatility being able to accommodate in the interlayer space a high loading of different dyes.[4] In numerous papers we and others have shown that g-ZrP (Fig. 1) is an excellent chemical support that different organic components can join leading to organic-inorganic materials with various properties.[5] Specifically, the phosphate-phosphonate topotactic exchange of g-ZrP with phosphonates derived from $Ru(bpy)_3$ and viologens allowed us the checking of these materials as DSSCs. Our studies showed that g-ZrP behaved as semiconductor and that this layered salt also exhibited a weak but useful photovoltaic response.[4] With the purpose of understanding the origin of the photovoltaic activity, laser flash photolysis and photo response spectrum were performed.[6,7] Both techniques surprisingly hinted that charge separation in the g-ZrP-based DSSCs was not promoted by light absorption of the dye, but by direct excitation of g-ZrP, the grafted dyes merely acting as electron acceptor/donor termini. One of the possible reasons for this odd behavior could be the achieved low loading of the included guests and/or the inappropriate orientation of the orbitals of the covalently grafted dyes with respect to the g-ZrP sheets.

In the present manuscript we report that by the appropriate incorporation of a suitable photo responsive donor–acceptor dyad into g-ZrP it is possible to prepare a DSSC that holds considerable promise for future development of more efficient cells based on an alternative mineral support to the classical TiO_2.

Results and discussion

Material preparation

With the aim of improving the photovoltaic response of g-Zr-based DSSCs and to provide further insight into the photo excitation phenomenon, in the present work we have studied a series of eight g-ZrP materials containing $Ru(bpy)_3^{2+}$ complexes that are expected to act as the light-harvesting component, and a viologen that could assist the process of charge separation. Yet, hereby, we should stress that both $Ru(bpy)_3^{2+}$ and the viologen are simply intercalated (*not covalently bonded*) into the intergallery spaces of g-ZrP (Fig. 2).

The active species are thus held between the lamellae by ionic forces. This simplifies considerably the preparation of these g-ZrP materials which can readily be made from commercially available $Ru(bpy)_3^{2+}$ and viologens without the need of appending them with the phosphonate groups required for the topotactic phosphate-phosphonate exchange reactions. At the same time, higher loadings of the active species can effortlessly be attained which will also enjoy more degrees of freedom in their relative arrangement between the inorganic layers, thus over- coming the main limitations detected in the previously studied ''covalent'' materials. Finally, the dyad $Ru(bpy)_3$-$(CH_2)_4$-Paraquat (Fig. 2, bottom) was synthesized to assure that both active components are linked and therefore enter the interlayer space in 1 : 1 ratio.

Table 1 summarizes the composition of the intercalation materials as determined by elemental analysis and ICP-MS. Table 1 also includes the interlayer distances measured by XRD.

The uptake of active species depends on the synthesis method. Material 1 was prepared by mixing 0.4 eq. of $Ru(bpy)_3$ and 0.2 eq. of MD (Fig. 2) with 1 eq. of g-ZrP, previously exfoliated in 1 : 1 water-acetone at 80 °C. It may be seen in Table 1 that the layered salt shows higher affinity for the viologen, even though it was the minor component, incorporating 15 molecules of it and only 8 of Ru complex. In order to increase the uptake of the Ru complex, materials 2–4 were then prepared in a sequential process, first treating exfoliated g-ZrP in 1 : 1 water-acetone at 80 °C with 0.3 eq. of $Ru(bpy)_3$ and isolating the resulting material that ended up intercalating 16–17 complex units with an interlayer distance of 1.96 nm (Fig. 3). Each of three portions of it was treated with 0.4 eq. of D, MD or P, leading respectively to materials 2, 3 and 4. Neither the starting amount of $Ru(bpy)_3$ nor the interlayer distance were altered by the second intercalation process which rendered a modest uptake of 6 viologen molecules (Table 1).

$Ru(bpy)_3$ may be considered as a sphere whose cross-section occupies *ca.* 1.5 nm^2. Therefore, taking into account that the total available space in a model sheet of 10 × 10 phosphates is *ca.* 30 nm^2 (Fig. 1), in principle, there should be room for *ca.* 20 units of Ru complex per 100 Zr, *i.e.* one phosphate every other five may interact with a $Ru(bpy)_3$ molecule. The experimental uptake is thus close to the theoretical one based on these simple geometrical grounds. The scarce remaining area (*ca.* 4.5 nm^2) should thus be made available for the viologen. The bipyridinium cross-section is highly dependent on orientation, the largest (0.65 nm^2) achieved when placed flat parallel to the layers. These simple calculations render space enough for 7 viologen molecules which fairly correspond to the factual uptake.

In order to get a more evenly leveled amount of the active components we established two different approaches. The simplest one was to repeat the sequential intercalation with third the amount (0.1 eq.) of Ru complex employed in the previous series of materials 2–4. This led to a starting material with only 10 molecules of $Ru(bpy)_3$. Treatment of three portions of it with 1.2 eq. of D, MD or P rendered materials 5, 6 and 7,

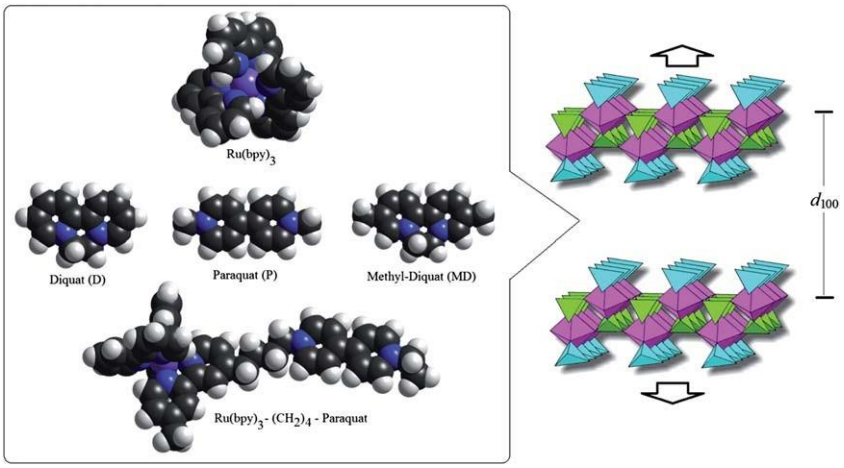

Fig. 2 Schematic view of the intercalated molecules within g-ZrP whose native basal space (1.20 nm) must increase as measured by powder XRD (see Table 1).

Table 1 Composition and interlayer separation of the g-ZrP intercalated samples studied in this work

	MOLECULAR FORMULA $[Zr(PO_4)(H_2PO_4)]_{100}[Ru(bpy)_3]_x(viologen)_y(H_2O)_a(C_3H_6O)_b$				
Material	X	y[a]	A	b	d_{100}[b](nm)
1	8	15 (MD)	200	0	1.65
2	17	6 (D)	200	0	1.92
3	16	6 (MD)	200	0	1.92
4	16	6 (P)	200	0	1.93
5	10	7 (D)	180	43	1.81
6	10	8 (MD)	200	35	1.78
7	10	7 (P)	150	40	1.78
8	11[c]	11[c]	210	0	1.92

[a] See Fig. 2 for abbreviations. [b] Measured from XRD of the corresponding materials (see supplementary material†). [c] $Ru(bpy)_3$-$(CH_2)_4$-Paraquat dyad (Fig. 2).

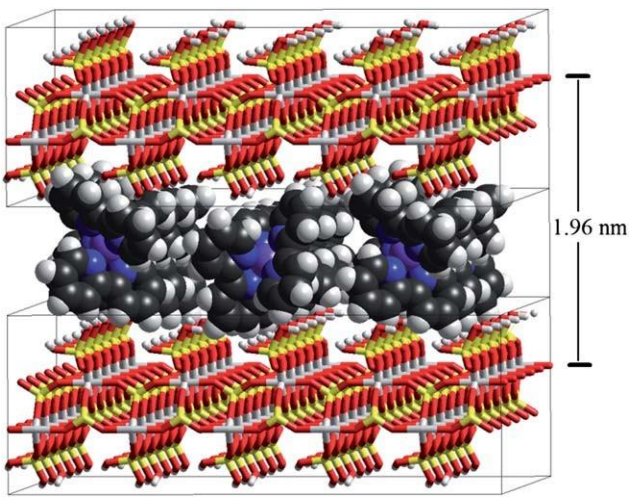

Fig. 3 Molecular model of a portion of g-ZrP intercalated with Ru(bpy)$_3$ at the experimental interlayer distance.

correspondingly, whose viologen uptake was of 7–8 molecules (Table 1), nearly the same as before. In these cases, in order to comply with the experimental analyses, we found it necessary to consider *ca.* 40 acetone molecules which should be occupying the empty space left respect to the analogous materials 2–4, the interlayer distance of materials 5–7 being a bit shorter (1.8 nm) than that of their counterparts (1.9 nm).

The second approach required some synthetic effort to prepare the $Ru(bpy)_3$-$(CH_2)_4$-Paraquat dyad. The literature shows that the use of dyads may be advantageous from the photochemical point of view to improve charge separation[8,9] and from the overall efficiency of the dyes in DSSCs.[3,10] Scheme 1 shows the synthetic procedure.

Exfoliated g-ZrP in the usual conditions was treated with 0.3 eq of the dyad. The uptake was of 11 molecules (see Table 1). The estimated cross-section of the dyad is *ca.* 3 nm^2 which allows for *ca.* 10 molecules inserted between model inorganic sheets of 10 × 10 phosphates, in excellent agreement with the experimental finding.

The primary event in the photovoltaic mechanism is the generation of electron and holes from light absorption. To measure the latter, diffuse reflectance UV-Vis spectra of the g-ZrP samples were recorded. Fig. 4 shows representative examples of these optical spectra to illustrate the type of bands that have been observed. Pristine g-ZrP exhibited a broad band from 200 to 330 nm. The band gap of this g-ZrP semiconductor was estimated from the onset of this absorption and was calculated to be 3.76 eV, corresponding to a wide band gap semiconductor. The samples containing Rubpy intercalated inside g-ZrP exhibited, in addition to the broad band due to the g-ZrP support, two additional peaks at 290 nm and 460 nm that match with the reported values of this metal complex, attributable to the ligand centered (290 nm) and metal-to-ligand (460 nm) electronic transitions. In addition, the bipyridinium ion introduces an extra absorption around 280 nm. Therefore it can be stated that the optical spectrum of the materials M1 to M8 consists in the combination of the bands corresponding to their individual components.

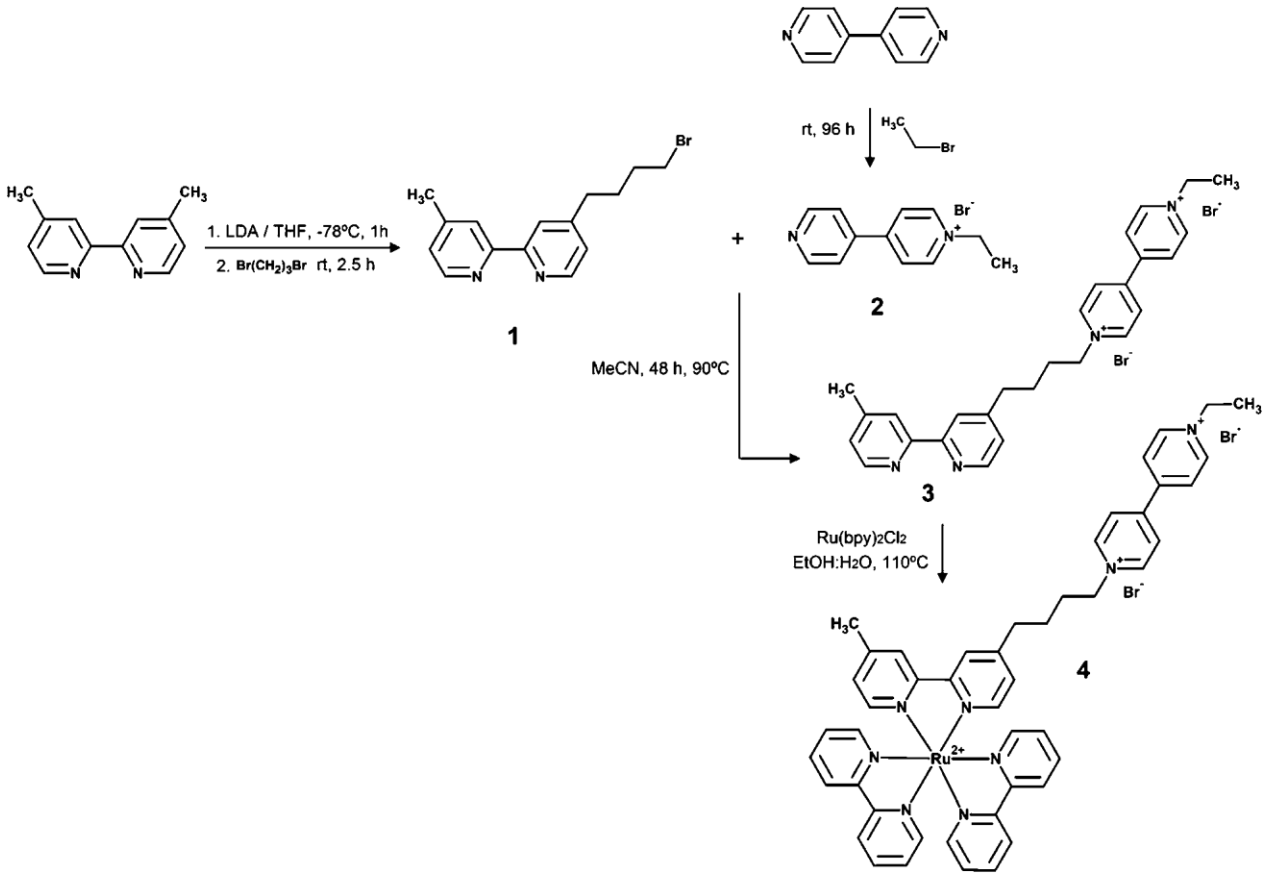

Scheme 1 Synthetic route followed to obtain $Ru(bpy)_3$-$(CH_2)_4$-Paraquat dyad.

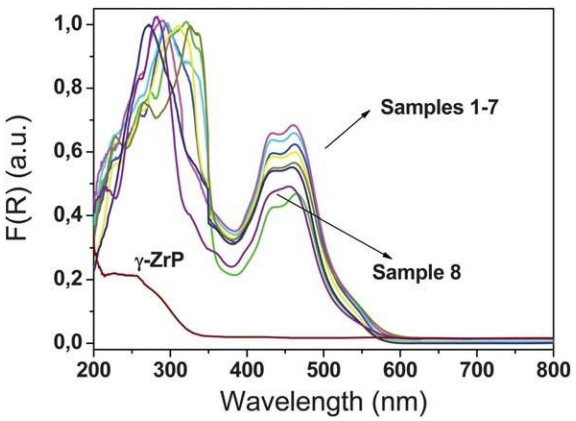

Fig. 4 Diffuse reflectance UV-Vis spectra of g-ZrP and samples 1 to 8.

Cyclic voltammetry of pure g-ZrP exhibited a reversible peak at —0.6 V corresponding to the reduction of the material (see Fig. 5). Observation of this reduction peak in cyclic voltammetry lends support to the possibility that upon excitation of Rubpy, its triplet excited state can inject an electron into the g-ZrP support, producing the reduction of the sites observed electrochemically. On the other hand, we proposed in previous work the possibility of current generation by direct excitation of g-ZrP. Herein we have determined the photocurrent intensity upon excitation of the pure g-ZrP phase from 300 to 500 nm (see insert in Fig. 5). In addition if a thin film of g-ZrP supported on FTO is submitted to a 0 V bias potential and the electrode illuminated at 300 nm, then, a photocurrent of about 0.5 mA can be measured (see right inset of Fig. 5). It can be seen that in fact a current was generated, thus, reinforcing the behavior of layered g- ZrP as

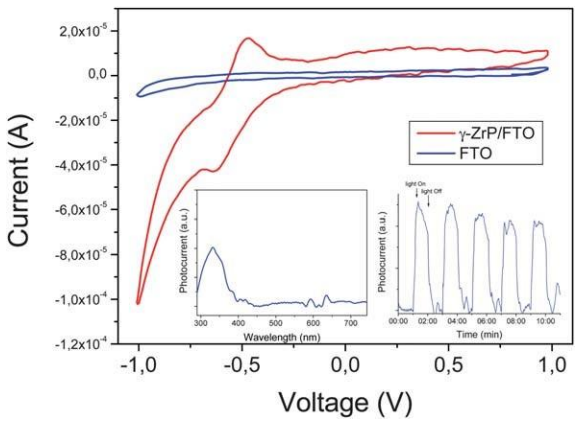

Fig. 5 Cyclic voltammetry of g-ZrP supported on FTO and FTO substrate as reference in a 0.1 M $LiClO_4$ acetonitrile solution. The left inset shows the photocurrent measured for this thin film of g-ZrP as a function of the excitation wavelength at 0 V bias potential. The right inset shows the photocurrent during repeated on/off cycles upon illumination with monochromatic light of 300 nm wavelength.

semiconductor with the photochemical generation of electrons and holes.

Further support of the semiconductor behavior of plain g-ZrP was obtained by performing the Mott-Schottky measurements of a thin film of this material supported on FTO electrode at 10 kHz. The results obtained (Fig. 6) from the electrode immersed in dry acetonitrile using $LiClO_4$ as electrolyte shows the typical behavior for a ''*n*'' type semiconductor. From the intersection of the linear fitting of the experimental points at the high positive voltages with the X axis a flat potential of —1.3 V *vs.* NHE electrode was estimated.

It is noteworthy that the flat potential of g-ZrP conduction band (—1.3 V) is far more negative than the reduction peak observed in CV (—0.6 V) and, therefore, it can be inferred that the electrochemical process does not correspond to the filling of the conduction band of g-ZrP semiconductor. Most probably, the CV peak would indicate the existence of interband states.

Photovoltaic measurements

The DSSCs were prepared by spreading a micrometric film of a paste of the corresponding materials 1–8 (see Table 1) onto a transparent FTO electrode. The average thickness of the dry films after removing the solvent and the organic additives of the paste was 6 mm, measured by an Ambios Xi-100 Non-Contact Optical Profilometer. It should be noticed that the procedure used to build these DSSCs does not include sintering by calcination as it is usual in the most efficient titania DSSCs, since the required temperature would irreversibly damage the organic-inorganic layered composite. Besides, in the case of TiO_2 high temperature sintering is necessary because the amorphous phase (photo chemically inefficient) has to be transformed into anatase, more efficient photo chemically speaking. In the case of g-ZrP we are dealing with the active species already from the start. For this reason the paste used for the film of the photoactive material was obtained using terpineol and removing it at 150 °C what may be considered as a low-temperature sintering process. Cellulose could not be used because the biopolymer requires higher temperature to be removed from the film.

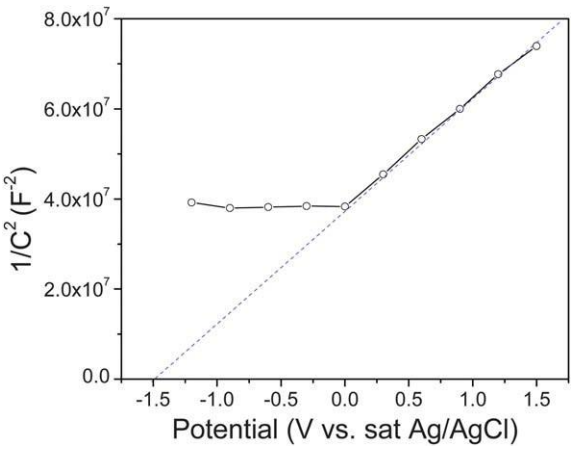

Fig. 6 Mott-Schottky plot of g-ZrP film recorded at 10 kHz in acetonitrile solution of 0.1M $LiClO_4$.

The results of the photovoltaic measurement are summarized in Table 2, while Fig. 7 presents some representative J-V plots for these cells. From the data shown in the Table 2 and Fig. 7, and comparing with our reported values for previous ''covalent'' g-ZrP materials,[4] it can be concluded that the present cells have much higher open circuit voltage (V_{OC}).

Table 2 and Fig. 7 show very consistent V_{OC} values for all the samples (*ca.* 0.5 V) that may be attributed to the difference in the redox potential of the I^-/I_3 couple and the Fermi level of the conduction band of the g-ZrP shared by all the samples. The short circuit density current (J_{SC}) appears to be independent on the $Ru(bpy)_3$ loading for the range under study. For instance, samples with more than double $Ru(bpy)_3$ dye content and similar electron relay viologen exhibit essentially the same efficiency regardless the $Ru(bpy)_3$ loading (see Table 2). Also the viologen content does not exert a significant influence on the J_{SC} in the range of loading under consideration.

With respect to the viologen, the influence of its nature (D, P or MD) on the performance of the g-ZrP based DSSC is relatively minor.

The fill factor (FF in Table 2) of all the cells was also very similar in the range of 0.35–0.4, probably due to the similar electrical resistance of the g-ZrP film in the series.

The data presented in Table 2 show that the solid g-ZrP intercalated with the dyad is by far the most efficient semiconductor, rendering a current density about four times higher than that of the other samples. Moreover, compared to our previously studied ''covalent'' materials M1 and M2,[4] the photovoltaic activity of the dyad-containing material 8 is *ca.* 20 times more efficient. Concerning the absolute efficiency of the DSSCs prepared with material 8 as photoactive material, the power conversion efficiency (PCE) is 0.1%. Although still far from the current efficiencies of titania based DSSCs with V_{OC}, J_{SC} and FF values of 0.7 V, 20 mA\$cm^{-2} and 70%, respectively, one should be aware that our materials have been prepared from plain $Ru(bpy)_3$ complex. It is well-documented in the field that the overall performance of the DSSC strongly depends on the nature of the dye and that the currently most efficient DSSCs are those prepared with N3[10] or black dye.[11] We are working along these lines highly encouraged by the results reported in this paper that represent an important leap forward in efficiency improve- ment from this interesting new application of the semiconducting properties of g-ZrP.[4] Taking into account the flexibility in the preparation of g-ZrP and the large variety of dyes and electron relays that can be incorporated, our present report could eventually open the way to achieve efficiencies with g-ZrP hopefully higher than those that can be obtained using TiO_2.

Photoresponse spectra

The main reason for the efficiency improvement observed for material 8 is in fact the photosensitization of the g-ZrP sheets by the $Ru(bpy)_3$-paraquat dyad. In contrast, the photocurrent spectra of materials 1–7 did not show, as it was earlier noticed, a clear band corresponding to the $Ru(bpy)_3$, indicating that the photovoltaic response did not arise upon excitation of the ruthenium complex in those materials (Fig. 8). It should be noted that materials 1–7 all exhibited the characteristic $Ru(bpy)_3$ absorption band at 460 nm in the visible region (Fig. 4). Yet, no

Table 2 Performance of DSSCs prepared with the g-ZrP samples 1–8 upon illumination with a solar simulator through a 1.5 AM filter at 1000 W$m^{-2}. V_{OC}: voltage at open circuit; J_{SC} current density at short circuit; FF: fill factor. For the sake of comparison the reported efficiency parameters of materials M1 and M2 previously studied by us are also included

Material	$Ru(bpy)_3$/viologen ratio	V_{OC} (V)	J_{SC} (mA$cm^{-2})	FF (%)
1	8 : 15	0.442	103	33.5
2	17 : 6	0.439	106	41.7
3	16 : 6	0.441	93	38.0
4	16 : 6	0.450	120	37.4
5	10 : 7	0.434	75	39.2
6	10 : 8	0.412	108	35.5
7	10 : 7	0.484	37	38.6
8	11 : 11	0.436	332	54.0
M1[a]	4 : 7	0.086	7.5	0.32
M2[a]	4 : 7	0.093	16.8	0.33

[a] See ref. 4

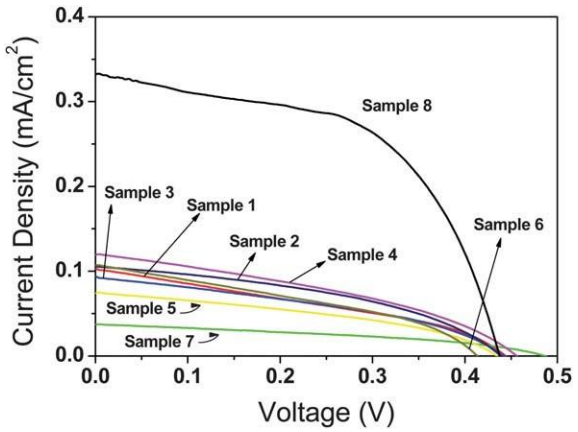

Fig. 7 Current density-voltage characteristics for L-ZrP DSSCs measured under simulated AM1.5 solar irradiation (1000 W$m^{-2}).

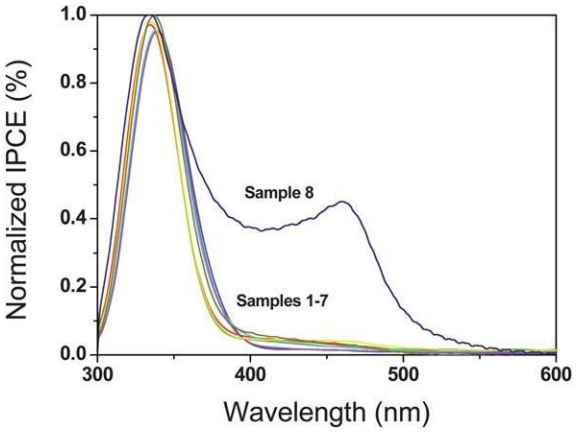

Fig. 8 Normalized IPCE spectra for g-ZrP-based DSSCs.

photovoltaic response in this region was observed. This lack of photovoltaic response upon irradiation at the absorption band of the ruthenium complex can explain why an increment in the loading of the latter dye was not concomitant with a photocurrent increase. This is even more puzzling considering that cyclic voltametry of g-ZrP (Fig. 5) showed that an electron in the triplet state of $Ru(bpy)_3$ must have enough energy to reduce g-ZrP.

Fortunately, in clear disparity to the behavior of materials 1–7, in which the ruthenium complex and the viologen are not forming a dyad, material 8 exhibited a photo response spectrum neatly consistent with the generation of photocurrent upon excitation of the dyad's $Ru(bpy)_3$ moiety, thus acting now as the intended light harvester. Fig. 8 shows the photoresponse spectrum recorded for material 8. This photo response partially explains the higher efficiency of the DSSC prepared with the material 8.

The behavior of 8 suggests that, for the $Ru(bpy)_3$ to act as the photosensitizer, it is needed the viologen relay stay close, something that cannot be assured in materials 1–7 where the active species are scattered and disordered along the intergallery space. In this regard, considering the reduction potential of viologens (—0.4 till —0.6 V) it seems energetically unfeasible that the viologen radical cation resulting of the photoinduced electron transfer from ruthenium tris(bipyridyl) in its excited state will inject an electron to the g-ZrP conduction band (—1.3 V). It seems, however, thermodynamically more reasonable that the electron of reduced viologen could be injected into the reduction peak observed in CV (—0.6 V) and, therefore, these interband sites are presumably those that are playing the key role in the photoelectrochemical response. Scheme 2 summarized the proposal.

Transient photo voltage measurements

The temporal profiles of the transient photo voltage upon exposure of the DSSCs to 532 nm laser pulse may provide further understanding of the measured efficiencies (Fig. 9).[12,13] The

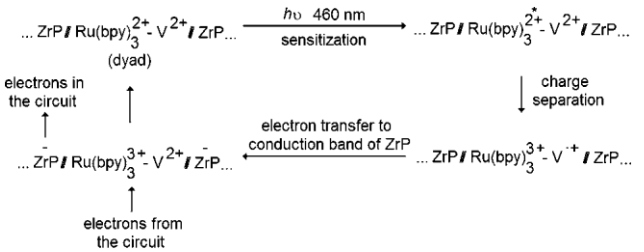

Scheme 2 The overall photoresponse of material 8. The most probable sites of electrons in ZrP are the interband states observed in CV.

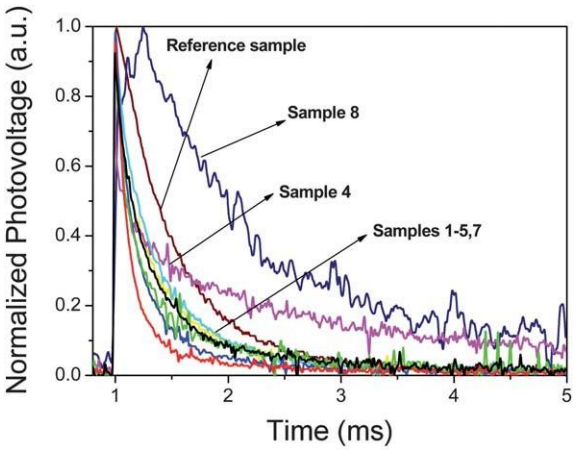

Fig. 9 Normalized transient photo voltage spectra for g-ZrP-based DSSCs.

Figure shows that the cell built from material 8 gave much longer-lived voltage exhibiting a significant rise in the first 500 ms after excitation. We interpret this growth as a consequence of the longer lifetime of the charge separation state in the ruthenium dyad (Scheme 2). Thus, excitation of this donor–acceptor dyad would lead to an instantaneous charge separation that will subsequently transfer with some delay the electron and hole to the g-ZrP semiconductor and I_3^- electrolyte, respectively. The voltage temporal profile of the DSSCs built with material 8 contrasts with those recorded for the other samples that do not exhibit the delayed growth and in addition they decay much faster. In this context it is interesting to comment that the second most efficient DSSC, the cell prepared with material 4, exhibited also the second longest voltage lifetime. Thus, the results of transient photo voltage correlate well with the efficiency of the DSSC built with g-ZrP, those with the slower transient photo voltage decay being the most efficient.

Conclusions

In the present work we have shown that the facile intercalation of dyad 4 (Scheme 1) into g-ZrP led to DSSCs of reasonable efficiency containing simple $Ru(bpy)_3$ and viologens in the inter-gallery space. Similar materials can easily be obtained by sequential intercalation of the separate active components into exfoliated g-ZrP nano sheets by extremely simple procedures. The ratio of the guests can effortlessly be controlled by variation of the concentration of the compounds in the solution. Photovoltaic cells based upon these g-ZrP samples exhibit very similar V_{OC} values and quantum efficiency, regardless of the loading of Ru dye and viologen, due to the surprising fact that sensitization from the dye to the g-ZrP nano sheets does not occur. The semiconducting properties of g-ZrP were supported by cyclic voltammetry, observation of photocurrent and Mott-Schottky measurements of thin films of this material supported on FTO electrode. The maximum efficiency obtained using these g-ZrP-based materials was obtained for the dyad 4 where the $Ru(bpy)_3$ complex was tethered to the viologen by a four-methylene bridge reaching a 0.1% that means a 20-fold enhancement with respect to our initial reports. This important improvement can bring these versatile layered materials to efficiencies even higher to those reached with DSSCs based on titanium dioxide. In particular, alternative dyes and preparation procedures that could allow sintering of the nanosheets to the electrode can lead to additional improvements. Efforts in this direction are currently being undertaken.

Experimental section

Materials

The complex $Ru(bpy)_3Cl_2$ and viologens D, MD and P (Fig. 2) were purchased from Aldrich and used as received.

Preparation of the dyad

Its preparation was accomplished as indicated in Scheme 1 (see numbers for the intermediates).

4-(4-bromobutyl)-4′-methyl-2,2′-bipyridine (1). Butyl lithium (1 M in hexanes, 2.7 mL, 4.34 mmol) was added to a solution of diisopropylamine (0.61 mL, 4.34 mmol) in 9 mL of THF at 78 °C, the mixture was stirred for 45 min and added to a solution of 4,4′-dimethyl-2,2′-bipyridine (1 g, 5.43 mmol) in 38 mL THF at the low temperature. After 1 h at —78 °C the resulting brown-red solution was treated with dibromopropane (0.88 mL, 8.69 mmol) and after stirring for 1 h a pale-green color was developed. The mixture is allowed to reach r.t. for 3 h and the reaction was quenched with water. Phosphate buffer (1M, 10 mL, pH 7.0) was added and the mixture was extracted with diethyl ether. Usual work-up of the organic yielded a crude product that was purified by silica-gel chromatography with 1 : 1 ethyl ether:hexane rendering a colorless oil 0.69 gr (41.5%). ^{1}H-NMR (300 MHz, $CDCl_3$) d (ppm): 1.89 (m, 4H), 2.44 (s, 3H), 2.74 (t, *J* ¼ 7.3 Hz, 2H), 3.42 (t, *J* ¼ 6.6 Hz, 2H), 7.14 (d, *J* ¼ 1.4 Hz, 2H), 8.24 (s, 2H), 8.54 (d, *J* ¼ 5.2 Hz, H), 8.57 (d, *J* ¼ 5.1 Hz, H); ^{13}C-NMR (75 MHz, $CDCl_3$) d (ppm): 156.0, 156.0, 152.9,148.9, 148.8, 148.1, 124.6, 123.9, 122.0, 121.3, 35.5, 34.0, 32.8, 30.4.

1-Ethyl-4-pyridin-4-ylpyridinium bromide (2). In a sealed tube a mixture of 4,4′-bipyridine (5 g, 32.0 mmol) and 2.6 mL of bromoethane (32.0 mmol) were stirred at room temperature for 96 h rendering a pale-yellow solid that was filtered and washed with diethyl ether, toluene and acetone. The remaining solid was dissolved in acetonitrile, the solution filtered and the solvent evaporated. Yield (85%). ^{1}H-NMR (300 MHz, DMSO) d (ppm): 1.57 (t, *J* ¼ 7.3 Hz, 3H), 4.71 (q, *J* ¼ 7.3 Hz, 2H), 8.05 (m, 4H), 8.65 (d, *J* ¼ 6.8 Hz, 2H), 8.84 (m, 2H), 9.31 (d, *J* ¼ 7.1 Hz, 2H). ^{13}C-RMN (75 MHz, DMSO) d (ppm): 16.29, 55.89, 121.85, 125.31, 140.82, 145.09, 150.87, 152.08.

1-Ethyl-1′-[4-(4′-methyl-2,2′-bipyridin-4-yl)butyl]-4,4′-bipyridinium dibromide (3). A mixture of 1 (309 mg, 1.03 mmol) and 2 (290 mg, 1.08 mmol) in 10 mL of CH_3CN was heated at 90 °C for 48 h in a sealed tube. The resulting yellow precipitate is filtered off and washed with hot CH_3CN and diethyl ether yielding 300 mg (52%) of the product. ^{1}H-NMR (300 MHz, DMSO) d (ppm): 1.60 (t, *J* ¼ 7.4 Hz, 3H), 1.71 (m, 2H), 2.04 (m, 2H), 2.40 (s, 3H), 2.77 (t, *J* ¼ 7.5 Hz, 2H), 4.74 (m, 4H), 7.29 (m, 2H), 8.22 (d, *J* ¼ 7.1 Hz, 2H), 8.52 (dd, *J* ¼ 4.8 Hz; 15.6Hz, 2H), 8.78 (d, *J* ¼ 4.9

Hz, 4H), 9.41 (d, J ¼ 6.5 Hz, 4H); ^{13}C-NMR (75 MHz, DMSO) d (ppm): 16.27, 20.68, 26.21, 30.27, 33.80, 56.52, 60.58, 120.45, 121.21, 124.15, 124.89, 126.51,126.61, 145.57, 145.73, 147.91, 148.48, 148.54, 148.90, 149.15, 151.46, 155.04, 155.30.

Dyad (4). A mixture of 3 (300mg, 0.526mmol) and *cis*-bis(2,2^0-bipyridine)dichlororuthenium (331mg, 0.684mmol) in 24 mL of 7 : 3 etanol:water for 24 h was heated at 110 °C protected from ambient light. The mixture was concentrated *in vacuo* to yield 631 mg of a dark solid which was used to prepare material 8 without further purification. ^{1}H-NMR (300 MHz,CD_3OD) d (ppm): 1.73 (t, J ¼ 7.5 Hz, 3H), 1.92 (m, 2H), 2.24 (m, 2H), 2.59 (s, 3H), 2.97 (m, 2H), 4.85 (m, 4H), 7.32 (d, J ¼ 5.7 Hz, H), 7.41 (d, J ¼ 5.7 Hz, H), 7.44–7.56 (m, 4H), 7.59 (d, J ¼ 5.7 Hz, H), 7.64 (d, J ¼ 5.9Hz, H), 7.78–7.87 (m, 4H), 8.07–8.17 (m, 4H), 8.65–8.75 (m, 10H), 9.28 (d, J ¼ 6.4 Hz, 2H), 9.34 (d, J ¼ 6.4Hz, 2H); ^{13}C-NMR (75 MHz, CD_3OD) d (ppm): 16.86, 21.32, 27.48, 31.87, 35.24, 58.64, 62.70, 125.66, 125.91, 126.70, 128.33, 128.87, 128.92, 128.98, 129.16, 129.78, 139.01, 146.81, 147.10, 151.11, 151.52, 151.85, 151.92, 152.49, 152.54, 155.07, 157.82, 158.09, 158.33, 158.37, 158.45.

General procedure of intercalation. 400 mg of g-ZrP was suspended in 40 mL of a mixture of water/acetone (1 : 1) and the suspensión was stirred at 80 °C for 35 min to attain complete exfoliation of the layers. The intercalate was dissolved in 33.4 mL of a mixture of water/acetone (1 : 1) and added to the g-ZrP suspension. The mixture was maintained 72 h at 80 °C and the solid was centrifuged, washed tree times for 20 min with distilled water and centrifuged again. The resulting orange solid was dried in the oven at 100 °C for 24h and conditioned at least 3 h in a desiccator containing a saturated solution of $BaCl_2$.

Diffuse reflectance UV-Vis spectra

Optical spectra in the 200–800 nm region were recorded for powdered samples by the diffuse reflectance mode using an integrated sphere. $BaSO_4$ was used as reference. The remittance (R) from the instrument was recorded the spectra plotted as the Kubelka-Munk function (F(R) ¼ (1 — R)^2/2R). The band gap of g-ZrP was estimated from the onset of the absorption band (330 nm) applying the equation: E (eV) ≥1240/l(nm)

Cell preparation

A series of photoelectrochemical cells were prepared by depositing a micrometric layer of the corresponding g-ZrP materials 1–8 onto a conducting transparent electrode FTO (Fluorine-doped tin oxide), using the doctor blade technique. The surface of the FTO electrode in which the film is deposited is defined by means of two parallel adhesive Scotch tapes. The final area obtained was 1 × 1 cm^2. The film was dried at 150 °C for 15 min to remove the terpineol from the paste. The platinized counter electrode was fabricated by thermal decomposition of H_2PtCl_6 isopropanol solution.[14] The ZrP electrode was assembled with the platinized transparent conducting glass using a double-sided adhesive polymer film (Surlyn, DuPont) that acts as separator and sealing element. The two electrodes were held together by hot melting the of Surlyn seal at 100 °C while applying pressure. The electrolyte (0.5M lithium iodide and 0.05M iodine in methoxypropionitrile) was introduced into the cell through the two holes which were drilled in the counter electrode.[15]

Characterization of g-ZrP as semiconductor

To provide the evidence supporting the semiconductor properties of g- ZrP three types of measurements on thin films of this material on FTO electrode, namely, cyclic voltammetry, photocurrent measurements and Mott-Schottky characterization were carry out. A FTO electrode coated by a thin film of g- ZrP prepared by doctor blade as described in the previous section was immersed in a 0.1 M $LiClO_4$ acetonitrile solution. The solution was purged with N_2 for at least 30 min before measurements. This electrode was connected to an AMEL 7050 potentiostate that allows us scan the voltage while measuring the current. Cyclic voltammetry was performed a scan rate of 20mV/s using a three electrode standard configuration with a platinum wire as counter electrode and Ag/AgCl sat. as reference electrode. The photocurrent spectrum was obtained by illuminating the g-ZrP FTO electrode with the monochromatic light from a xenon lamp using a Czerny–Turner monochromator. The intensity in current was transferred to a PC with the appropriate software to control the experiment and handle the data. Similarly, the photocurrent was determined during repeated on/off cycles of monochromatic 300 nm light at 0 V bias potential. The Mott-Schottky measurement was carry out by immersing a thin film of g-ZrP supported on FTO electrode in a 0.1M $LiClO_4$ acetonitrile solution. The capacitance measurements were carried out at 10 kHz within the potential range from +1.5 to —1.2 V (*versus* a Ag/AgCl reference electrode) using a frequency response analyser (AMEL, model 7200) connected to the AMEL 7050 potentiostate.

Photovoltaic response measurements

To determine the J-V plots, the cell was connected to a source-Meter (Keithley 2601) by using metallic clamps covered with gold. The voltage scan was controlled using ReRa Tracer software. The data was automatically transferred to a PC that controlled the experiment and at the same time provided data-storage capability to the system. The solar simulator (Sun 2000, ABET Technologies) was adapted to the AM 1.5G filter and the nominal power for the measurements was 100 mW/cm^2. The same cells were used to record the IPCE spectra. The sample was excited with a 150 W xenon lamp through a Czerny–Turner monochromator. The current output at short circuit was measured by a potentiostat (AMEL), which transferred the data through the A/D converter to the PC controlling the monochromator apparatus. IPCE curves were calculated using a Newport (818-UV-L) calibrated photodiode.

Transient photovoltage

A pulsed Nd:YAG laser (Quanta-ray, Spectra-Physics, 532 nm, 8 ns pulse width) was used as excitation source for transient photovoltage measurements. The laser irradiated the cell from the side of ZrP film. Then photovoltage transients were recorded by connecting the cell directly to an oscilloscope (Tektronix, TDS

640A) that digitalized the response and transfer the data to a PC that controls the measurements and store the data.

Acknowledgements

The UPV-CSIC group is grateful to the Spanish MICINN for grant CTQ2009-11863. The UAM group thanks ERCROS-Farmacia S.A. for indirect funding and regrets that the financial backing from MICINN has been negated after the generous grants received in the near past (MAT2002-03243, MAT2006-00570).

References

1 M. R. Hoffmann, S. T. Martin, W. Y. Choi and D. W. Bahnemann, *Chem. Rev.*, 1995, 95, 69–96.
2 B. O'Regan and M. Gratzel, *Nature*, 1991, 353, 737–740.
3 M. Gratzel, *J. Photochem. Photobiol., C*, 2003, 4, 145–153.
4 L. Teruel, M. Alonso, M. C. Quintana, A. Salvador, O. Juanes, J. C. Rodriguez-Ubis, E. Brunet and H. Garcia, *Phys. Chem. Chem. Phys.*, 2009, 11, 2922–2927.
5 M. Ogawa and K. Kuroda, *Chem. Rev.*, 1995, 95, 399–438.
6 E. Brunet, M. Alonso, M. C. Quintana, P. Atienzar, O. Juanes, J. C. Rodriguez-Ubis and H. Garcia, *J. Phys. Chem. C*, 2008, 112, 5699–5702.
7 E. Brunet, M. Alonso, C. Cerro, O. Juanes, J. C. Rodr´ıguez-Ubis and Á. E. Kaifer, *Adv. Funct. Mater.*, 2007, 17, 1603–1610.
8 J. S. Krueger, J. E. Mayer and T. E. Mallouk, *J. Am. Chem. Soc.*, 1988, 110, 8232–8234.
9 Y. I. Kim and T. E. Mallouk, *J. Phys. Chem.*, 1992, 96, 2879–2885.
10 M. Gratzel, *J. Photochem. Photobiol., A*, 2004, 164, 3–14.
11 M. K. Nazeeruddin, P. Pechy, T. Renouard, S. M. Zakeeruddin, R. Humphry-Baker, P. Comte, P. Liska, L. Cevey, E. Costa, V. Shklover, L. Spiccia, G. B. Deacon, C. A. Bignozzi and M. Gratzel, *J. Am. Chem. Soc.*, 2001, 123, 1613–1624.
12 X. T. Zhang, H. W. Liu, T. Taguchi, Q. B. Meng, O. Sato and A. Fujishima, *Sol. Energy Mater. Sol. Cells*, 2004, 81, 197–203.
13 B. C. O'Regan, K. Bakker, J. Kroeze, H. Smit, P. Sommeling and J. R. Durrant, *J. Phys. Chem. B*, 2006, 110, 17155–17160.
14 N. Papageorgiou, W. F. Maier and M. Gratzel, *J. Electrochem. Soc.*, 1997, 144, 876–884.
15 A. N. M. Green, E. Palomares, S. A. Haque, J. M. Kroon and J. R. Durrant, *J. Phys. Chem. B*, 2005, 109, 12525–12533.

Authors Queries

Journal: EE

Paper: c1ee02158c

Title: Layered g-zirconium phosphate as novel semiconductor for dye sensitized solar cells: Improvement of photovoltaic efficiency by intercalation of a ruthenium complex-viologen dyad

Editor's queries are marked like this... 1, and for your convenience line numbers are inserted like this... 5

Query Reference	Query	Remarks
1	[INFO-1] For your information: You can cite this paper before the page numbers are assigned with: (authors), Energy Environ. Sci., DOI: 10.1039/c1ee02158c.	
2	Table of contents entry: If the entry does not fit between the two horizontal lines, then please trim the text and/or the title or perhaps abbreviate the authors' first names to initials.	